Relaxation Behavior of Polyimides Based on 2,2'-Disubstituted Benzidines

John C. Coburn,[*,†] **Paul D. Soper,**[‡] **and Brian C. Auman**[§]

DuPont Corporate Science and Engineering, Experimental Station, P.O. Box 80323, Wilmington, Delaware 19880-0323, DuPont Corporate Science and Engineering, Experimental Station, P.O. Box 80328, Wilmington, Delaware 19880-0328, and DuPont Electronics, Experimental Station, P.O. Box 80336, Wilmington, Delaware 19880-0336

ABSTRACT: The mechanical relaxation behavior of polyimides based on a variety of 2,2'-disubstituted benzidines and rigid dianhydrides was investigated. Two transitions were observed in these polyimides. The glass relaxation process is relatively weak and occurs at high temperatures due to the linear and rigid nature of these polyimides. The subglass relaxation is very prominent in these polyimides and is due to main-chain rotational motion localized within the diamine (benzidine) segment. Changes in the dianhydride moiety have little effect on the temperature of the subglass transition and result in only minor changes in the magnitude of this relaxation. The presence of 2,2'-CF_3 substituents on the benzidine moiety increases the magnitude and shifts the subglass relaxation approximately 150 °C to higher temperatures versus Cl or CH_3 in these positions. Incorporating a flexible ether linkage between the phenyl rings of the benzidine and the CF_3 side group (e.g., OCF_3) substantially reduces the temperature and to some extent the magnitude of the subglass relaxation. Replacement of the 2,2'-disubstituted benzidine unit (two phenyl rings) with one (benzene) or three (terphenyl) *unsubstituted* phenyl rings results in a substantial decline in both the temperature and magnitude of the subglass relaxation. Molecular modeling was used to clarify the nature of the subglass relaxation. Rotational energy barriers for the 2,2'-disubstituted benzidines, calculated from both semiempirical and density functional quantum mechanical calculations, are comparable in magnitude to the experimentally determined activation energies for the subglass relaxation.

Introduction

Polyimides are unique because of their high-temperature properties, chemical resistance, electrical characteristics, toughness, and dimensional stability. By adjusting their chemical structures, polyimides can be tailored to meet specific design criteria. For example, incorporating fluorinated groups into the polyimide generally reduces moisture absorption and the dielectric constant, critical for materials used in electronics. Since polyimides are frequently used as coatings or films adhered to metal or silicon substrates, low thermal expansion coefficients (TEC) that match those for the underlying substrates are desirable to reduce thermal stresses. Increasing the rigidity of the polyimide backbone by using highly linear (rodlike) monomers usually results in a low in-plane thermal expansion coefficient. To combine the desirable attributes of low dielectric constant, moisture absorption, and in-plane TEC, fluorinated, highly rodlike polyimides have now been developed.[1-4] One class of monomers that appears particularly useful in this regard is the 2,2'-disubstituted benzidines (2,2'-disubstituted-4,4'-diaminobiphenyl), especially 2,2'-bis(trifluoromethyl)benzidine[1,5-9] and 2,2'-bis(trifluoromethoxy)benzidine.[2,3]

Because of the backbone stiffness, polyimides containing 2,2'-bis(trifluoromethyl)benzidine have high glass transitions that are barely observable by thermal analysis. An uncommon feature of these polyimides is that they exhibit a rather prominent subglass relaxation.[10-13] In addition, this subglass relaxation generally occurs at much higher temperatures than typically observed in most other polyimides. The reason for the prominence and high temperature of the subglass relaxation is not well understood, in part because the nature of the subglass relaxation in polyimides is not fully understood. This relaxation in the well-studied polyimide pyromellitic dianhydride—4,4'-oxydianiline has been attributed to interplane slippage because this relaxation, which was observed in an oriented film, was not observed in an essentially unoriented molded sample.[14] Bernier et al.[15] attributed the subglass relaxation in polyimides to rotation of phenyl groups. Perena[16] attributed this relaxation to oscillations of the phenyl groups in the diamine residue.

In this paper, we investigated the mechanical relaxation behavior in rigid polyimides containing 2,2'-bis-(trifluoromethyl)benzidine in order to better understand the role of 2,2'-substituents on the relaxation behavior in this important class of polyimides. We also studied the relaxation behavior of several other 2,2'-disubstituted benzidine based polyimides with different side-group substituents and different dianhydrides. These results were also compared to analogous structures in which the 2,2'-disubstituted benzidine unit was replaced with either an unsubstituted phenyl or terphenyl moiety. The relaxation behavior was investigated primarily in terms of the temperatures, magnitudes, and frequency dependencies of the subglass process. Activation energies for the subglass transitions were calculated from the frequency dependence of these relaxations. The experimental results were complemented with computational modeling to determine possible molecular motions that could account for the subglass processes in these polyimides.

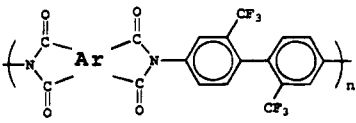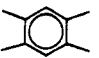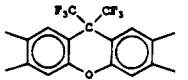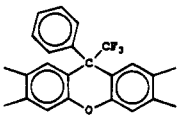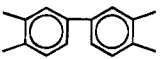* To whom correspondence should be addressed.
† DuPont Corporate Science and Engineering, Experimental Station, P.O. Box 80323, Wilmington, DE 19880-0323.
‡ DuPont Corporate Science and Engineering, Experimental Station, P.O. Box 80328, Wilmington, DE 19880-0328.
§ DuPont Electronics, Experimental Station, P.O. Box 80336, Wilmington, DE 19880-0336.

Table 1. Characterization of Polyimide Films Based on Various Rigid Dianhydrides and TFMB

Ar	Dianhydride Acronym	T_g (°C)	T_β (°C)	ΔH_{ACT}^β (kcal/mole)
	PMDA	ND	301	36.1
	6FCDA	424	302	35.9
	3FCDA	408	301	30.9
	BPDA	340	315	37.8

Table 2. Characterization of Polyimide Films Based on 6FCDA and 2,2'-Disubstituted Benzidines

R	Diamine Acronym	T_g^1 (°C)	T_β^1 (°C)	ΔH_{ACT}^β (kcal/mole)
-Cl	DClB	425	141	22.7
-CH₃	DMB	409	173	23.2
-CF₃	TFMB	424	302	35.9
-OCF₃	TFMOB	381	138	33.3
-OCF₂CF₂H	TFEOB	413	180	27.0
-OCF₂CFHO(CF₂)₂CF₃	DFPOB	ND	215	43.3
p-phenyl[2]	PPD	432	181	33.5
p-terphenyl[2]	DATP	436	175	35.6

[1]Transition temperatures were obtained from the maximum in the tan δ (@100 r/s) versus temperature curves.

[2] in polyimide structure is replaced by: for p-phenyl for p-terphenyl.
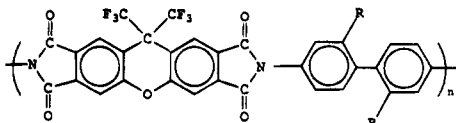
Experimental Section

Materials. The dianhydrides, 9.9-bis(trifluoromethyl)xan-thenetetracarboxylic dianhydride (6FCDA) and 9-phenyl-9-(trifluoromethyl)xanthenetetracarboxylic dianhydride (3FCDA), were prepared previously by Trofimenko.[17] Pyromellitic di-anhydride (PMDA) and 3,3′,4,4′-biphenyltetracarboxylic dian-hydride (BPDA) were polymer-grade commercial materials. All dianhydrides were dried at 150–180 °C under vacuum with N₂ bleed prior to use.

The diamines, 2,2′-dimethylbenzidine (DMB) and 2,2′-dichlorobenzidine (DClB), were obtained in high purity from sources within DuPont. The 2,2′-bis(trifluoromethyl)benzidine (TFMB, Marshallton) was sublimed and recrystallized from toluene prior to use. The 2,2′-bis(trifluoromethoxy)benzidine (TFMOB), 2,2′-bis(1,1,2,2-tetrafluoroethoxy)benzidine (TFEOB), and 2,2′-bis[2-(hexafluoropropoxy)-1,1,2-trifluoroethoxy]ben-zidine (DFPOB) were prepared by Feiring.[2,3] The 4,4′-diami-noterphenyl (DATP, Lancaster) was purified as described in ref 18. The p-phenylenediamine (PPD) was high-purity poly-mer grade from DuPont. All the diamines were dried at 50–80 °C under vacuum with N₂ bleed prior to use.
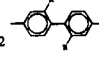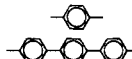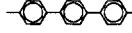
Polymer Synthesis. The polyimides were prepared by the standard room temperature synthesis of the poly(amic acid) from diamine and dianhydride monomers in N-methylpyrro-lidinone (NMP) with subsequent spin-coating and thermal cure to polyimide. A typical example is given as follows: A 100 mL reaction kettle fitted with a mechanical stirrer and nitrogen inlet and outlet was charged with 4.5231 g (9.8708 mmol) of 6FCDA and 3.4769 g (9.8708 mmol) of TFMOB. Shortly thereafter, 32 mL of NMP was added and stirring begun. 6FCDA dissolved slowly into the reaction mixture. The reaction was allowed to stir under nitrogen at room temper-ature overnight (ca. 18 h). The next day, a homogeneous, viscous, pale yellow solution resulted which was diluted to 16 wt % (from the original 20 wt %) with NMP. The solution was allowed to stir overnight (ca. 18 h) to allow for further equilibration. The following day, the poly(amic acid) solution was pressure-filtered through a 1 μm filter in preparation for spin-coating. The chemistries of the various polyimides synthesized for this study are shown schematically in Tables 1 and 2. The molecular weight characterization of these various polymers can be found elsewhere.[1–4,18]

Film Preparation. Films were prepared by spin-coating the filtered poly(amic acid) solution onto 5-in. silicon wafers containing 1000 Å of thermally grown oxide on the surface. The spin-coated wafers were dried in a convection air oven at 135 °C for 30 min. The dried wafers were then heated under

nitrogen at 2 °C/min to 200 °C and held for 30 min. The wafers were further heated under nitrogen at 2 °C/min to 350 °C and held for 1 h to complete conversion of the poly(amic acid) to the polyimide. All films were approximately 10 μm thick. The film thickness was controlled by adjusting the spin-coating speed. Free-standing films were obtained by etching the oxide layer of the silicon wafer in dilute aqueous HF to release the film. The basic mechanical, thermal, and electrical properties of these films were reported elsewhere.[1–4,18]

Measurements. Dynamic mechanical measurements were made using a Rheometrics RSA-II solids analyzer. The data were acquired with a dynamic strain amplitude of 0.1% using the frequency/temperature sweep mode. Data were obtained at 1, 10, and 100 rad/s at 5 °C temperature steps from room temperature to 500 °C. The decomposition temperatures for the polyimides in this study, reported elsewhere,[1,4] are above the glass transition temperatures and, therefore, are not expected to affect the dynamic mechanical behavior through the glass transition region.

The frequency-dependent modulus and loss modulus in the region of a relaxation process can be described in terms of the magnitude of the relaxation, $(E_u - E_r)$, and the distribution of relaxation times using the expressions 1 and 2, respectively.[19]

$$E'(\omega) = E_r + (E_u - E_r)\int_{-\infty}^{\infty} \frac{\varphi(\ln \tau)\omega^2\tau^2 \, d\ln \tau}{1 + \omega^2\tau^2} \quad (1)$$

$$E''(\omega) = (E_u - E_r)\int_{-\infty}^{\infty} \frac{\varphi(\ln \tau) \, \omega\tau \, d\ln \tau}{1 + \omega^2\tau^2} \quad (2)$$

where τ is the relaxation time, $\varphi(\ln \tau)$ is the relaxation time distribution function, and ω is the frequency. The tan δ is simply the ratio of the loss modulus to the modulus, $E''(\omega)/E'(\omega)$. Assuming Arrhenius behavior for the subglass relax-ation processes, the temperature dependence of the relaxation time constant, τ, can be given by the expression

$$\tau(T) = \tau_0 \exp(E_a/RT) \quad (3)$$

where E_a is the activation energy and τ_0 is the preexponential factor. Assuming a symmetrical distribution of relaxation
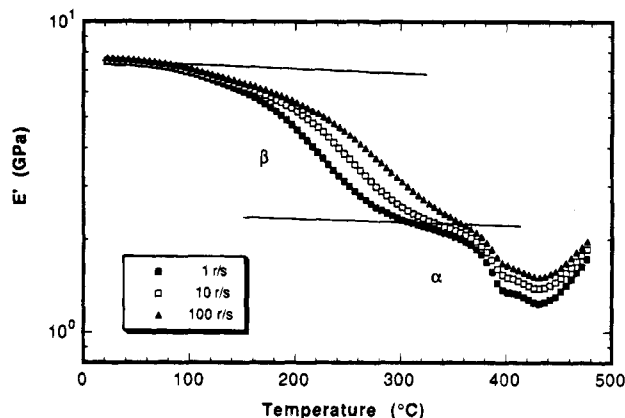
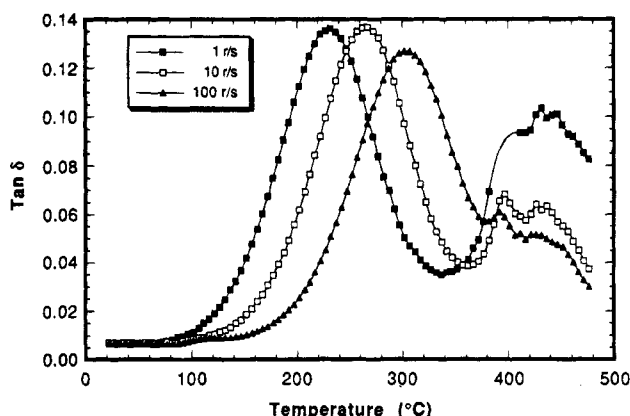**Figure 1.** Dynamic tensile modulus of 6FCDA/TFMB versus temperature at frequencies of 1, 10, and 100 rad/s.

Figure 2. Dynamic tan δ of 6FCDA/TFMB versus temperature at frequencies of 1, 10, and 100 rad/s.

Figure 3. Log(frequency) vs inverse temperature for the β subglass relaxation in 6FCDA/TFMB.

Figure 4. Dynamic tensile modulus (at 100 rad/s) of TFMB diamine based polyimides with different dianhydrides.

times, the tan δ is a maximum when $\omega\tau = 1$. Activation energies were determined from the slope of the log(frequency) versus inverse temperature plots. The transition temperatures were determined from maxima in the isochronal tan δ versus temperature curves.

Calculation Method. Semiempirical calculations were performed by using the MNDO93 program[20-22] with the MNDO/AM1 Hamiltonian.[22] Density functional calculations were performed by the DGAUSS program,[23-25] which employs Gaussian basis sets. The basis sets used for heavy atoms in this calculation are double-ζ in the valence space augmented with a set of polarization (d) functions. Optimizations were performed at the local density functional (LDFT) level with the local potential of Vosko, Wilk, and Nusair.[26] Single-point energies were calculated at the optimized geometries at the self-consistent gradient-corrected level with the nonlocal correlation functional of Perdew[27] and the nonlocal exchange potential of Becke[28-30] (NLDFT). All calculations were run with the UniChem 2.1 software from Cray Research, Inc., and were performed on a Cray YMP supercomputer.

Results and Discussion

Initially, the relaxation behavior of the control polyimide, 6FCDA/TFMB, was investigated. The dynamic tensile modulus and tan δ at frequencies of 1, 10, and 100 rad/s for the control polyimide are shown as a function of temperature from 25 to 500 °C in Figures 1 and 2, respectively. This fluorinated, nearly rodlike polyimide exhibits two relaxations. The high-temperature process observed at approximately 420 °C is attributed to the glass transition. This relaxation is not very prominent as evidenced by a small decrease in the dynamic modulus and a relatively small peak in the tan δ curve in the range of this transition. The subglass relaxation is observed in the 200–300 °C range and is
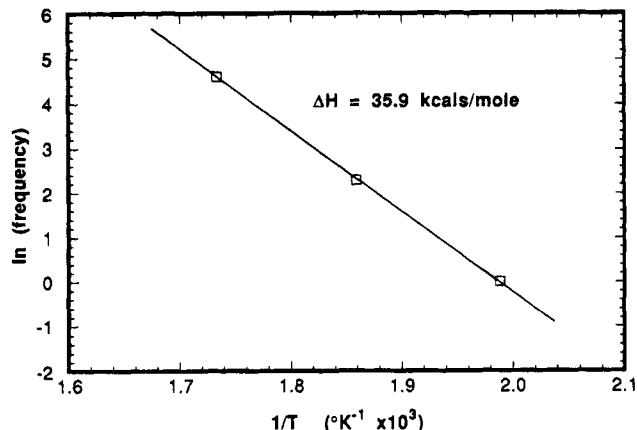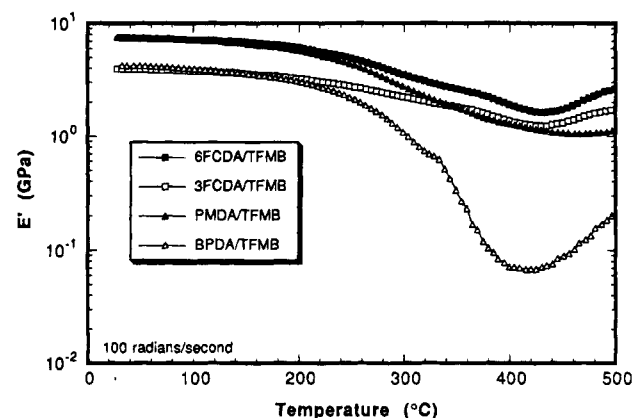
much more prominent than the glass relaxation. The subglass transition temperature is higher than normally observed in other polyimides.[15-16,31-36] The log(frequency) vs inverse temperature obtained from maxima in the tan δ versus temperature curves is shown in Figure 3. The activation energy of the subglass relaxation is 35.9 kcal/mol, characteristic of a subglass relaxation involving noncooperative localized motion.[37]

Next, the effect of dianhydride chemistry on the subglass relaxation was investigated. To this end, three different rigid dianhydrides, namely, PMDA, 3FCDA, and BPDA, were synthesized with TFMB. The dynamic tensile modulus and tan δ for this series of polyimides along with 6FCDA/TFMB are shown in Figures 4 and 5, respectively. The glass and subglass transition temperatures along with the calculated activation energies for the subglass relaxation are reported in Table 1. Because of the rigidity of the dianhydrides, the glass relaxation of three of the four polyimides is relatively small. The exception is the BPDA/TFMB polyimide where the somewhat less stiff BPDA (rotation about the C—C bond between the phenyl rings) increases the overall polymer chain flexibility and, in turn, the magnitude of the glass relaxation. The subglass relaxations are prominent, comparable in size, and occur at essentially the same temperature for all four polyimides. The insensitivity of the subglass temperature and magnitude to changes in the dianhydride is evidence that the subglass process is localized largely within the TFMB moiety. The less stiff BPDA appears to enhance the magnitude of the subglass relaxation. This apparent increase is attributed to the overlap of the promi-
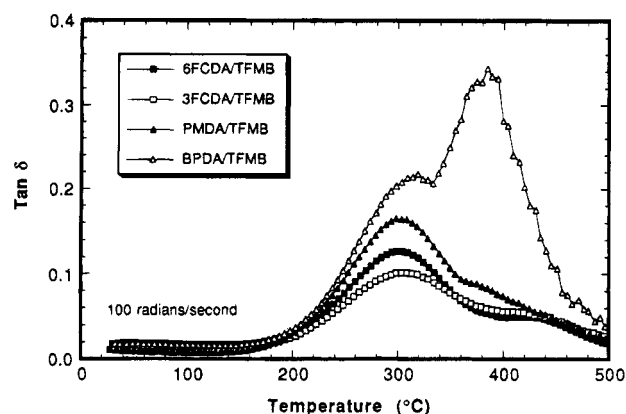
Figure 5. Dynamic tan δ (at 100 rad/s) of TFMB diamine based polyimides made with different dianhydrides.
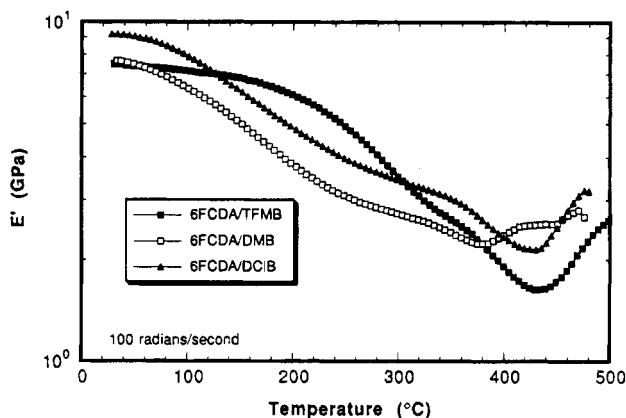

Figure 6. Dynamic tensile modulus (at 100 rad/s) of 6FCDA dianhydride based polyimides with diamines with different side group substituents.
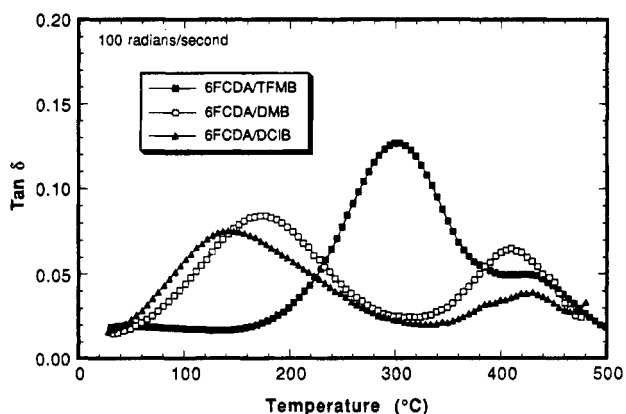

Figure 7. Dynamic tan δ (at 100 rad/s) of 6FCDA dianhydride based polyimides with diamines with different side-group substituents.

nent glass relaxation in this polyimide with the subglass relaxation.

Since the subglass relaxation was found to be unaffected by changes to the dianhydride chemistry, the effect of varying the 2,2'-substituents of the benzidine moiety on the subglass relaxation behavior was explored. The dynamic tensile modulus and tan δ for a series of polyimides based on the 6FCDA and the 2,2'-disubstituted benzidines with CF$_3$, CH$_3$, and Cl side groups are shown in Figures 6 and 7, respectively. Glass and subglass transition temperatures, along with the activation energies for the subglass relaxations, are included in Table 2. The glass relaxation for the three polyimides is small and occurs at about the same

Table 3. Dihedral Angles and Shortest Nonbond Distances of Minimum-Energy Structures

side-group substituent	semiempirical MO theory (MNDO/AM1)		local density functional theory	
	θ_{opt} (deg)[a]	shortest nonbond dist (Å)	θ_{opt} (deg)[a]	shortest nonbond dist (Å)
Cl	94	3.71	129	2.77
CH$_3$	103	2.62	123	2.33
CF$_3$	112	2.57	116	2.40
OCF$_3$	136	2.37	137	2.36
OC$_2$F$_4$H	128	2.54	b	b
OC$_2$F$_3$HOC$_3$F$_7$	126	2.57	b	b

[a] θ_{opt} = dihedral angle of minimum-energy structure. [b] Not calculated.

Table 4. T_β (°C) and Semiempirical and Density Functional Theory Rotational Energy Barriers (ΔE) in kcal/mol.

side-group substituent	semiempirical (AM1)		density functional theory	
	T_β	ΔE^a	ΔE(LDFT)[b]	ΔE(NLDFT)[b]
OCF$_3$	138	8.0	6.5	7.9
Cl	141	14.8	12.2	13.5
CH$_3$	173	19.3	12.8	14.9
CF$_3$	302	24.2	17.4	19.9

[a] ΔE = difference in energy between the minimum-energy structure and the structure with a dihedral angle of 180°. [b] ΔE = difference in energy between the LDFT minimum-energy structure and the LDFT structure with a dihedral angle of 180°.

temperature of approximately 420 °C. The subglass relaxation is prominent for all the 2,2'-disubstituted benzidines. Interestingly, the temperature and to a lesser extent the magnitude of the subglass process vary substantially with respect to the substituent. The temperature of the transition increases in the order Cl < CH$_3$ < CF$_3$. The increase in transition temperature in going from the CH$_3$ to the CF$_3$ groups is astounding; the subglass transition increases approximately 130 °C. This increase is attributed to the hindrance to rotation about the central C$-$C bond caused by the relative size increase of the substituents. This interpretation is supported by calculations of the rotational barrier at 180° of 2,2'-substituted biphenyls, which are discussed later in detail. The calculated rotational barriers are given in Tables 3 and 4. For small substituents, listed in Table 4, smaller rotational barriers correlate well with lower subglass transition temperatures.

The effects of incorporating a flexible ether linkage between the phenyl rings and the CF$_3$ 2,2'-substituents in the TFMB segment as well as increasing the length of the substituent were also explored. The dynamic tensile modulus and tan δ for polyimides based on the 6FCDA and 2,2'-disubstituted benzidines with CF$_3$, OCF$_3$, and fluoroalkoxy side-group substituents of different lengths are shown in Figures 8 and 9, respectively. The activation energies are reported in Table 2. The glass relaxation in all four polyimides is small, occurring at relatively high temperatures, due again to the highly rodlike polyimide backbone chemistry. The subglass relaxation is again dramatically affected by changes in the nature of the side group. Incorporating an ether linkage between the rings and the CF$_3$ groups dramatically *reduces* the subglass transition temperature over 150 °C from 302 to 138 °C. The oxygen attached to the phenyl ring acts as a "swivel", reducing the steric repulsion and the rotational energy barrier of the biphenyl rings. Further increasing the length of the fluoroalkoxy side group by incorporating additional
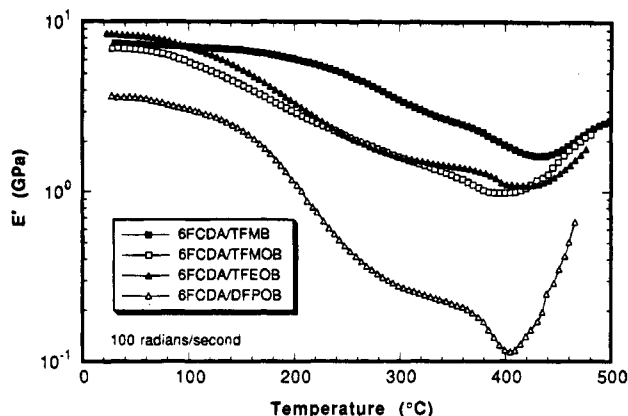
Figure 8. Dynamic tensile modulus (at 100 rad/s) of 6FCDA dianhydride based polyimides with diamines with different length side-group substituents.
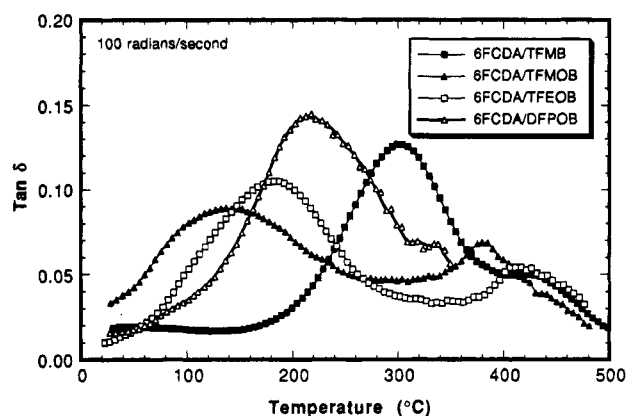

Figure 9. Dynamic tan δ (at 100 rad/s) of 6FCDA dianhydride based polyimides with diamines with different length side-group substituents.

Figure 10. Dynamic tensile modulus (at 100 rad/s) of 6FCDA polyimides made with different diamines.

Figure 11. Dynamic tan δ (at 100 rad/s) of 6FCDA polyimides made with different diamines.

CF_2 units and/or an additional ether linkage increases the temperature and magnitude of the subglass relaxation versus OCF_3, but still does not reach the temperature obtained for CF_3. The calculated rotational barriers of the ethers are listed in Table 3. The barriers are roughly the same regardless of the length of the side chain. The slight temperature increase with increasing substituent length is most likely due to interaction of the side group with neighboring polymer chains.

Since the subglass relaxation is believed to involve motion of the phenyl groups isolated to the diamine segment, changing the number of phenyl groups within this moiety on the relaxation behavior was also explored. The dynamic tensile modulus and tan δ for polyimides made with the 6FCDA dianhydride and with TFMB, PPD, and DATP diamines are shown in Figures 10 and 11, respectively. A comparison of the PPD and DATP polyimides with an analogous polyimide based on unsubstituted benzidine would obviously be more appropriate; however, due to the known toxicity and regulatory problems associated with benzidine, this comparison was not attempted. The activation energies are reported in Table 2. The glass relaxation is essentially equivalent for all three samples whether the diamine contains one (PPD), two (TFMB), or three (DATP) aromatic rings. All three diamines are, of course, rigid rodlike, and changing the length of the rod apparently has little effect on the chain flexibility or configuration and, in turn, the glass transition. On the other hand, the subglass relaxation for the *substituted* benzidine (two aromatic rings in the diamine) differs substantially from the other two *un*substituted samples.
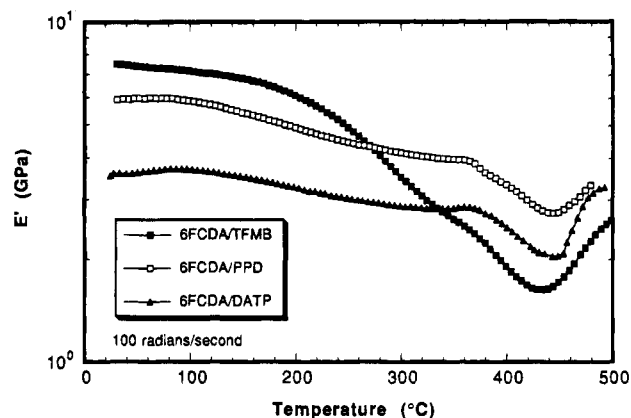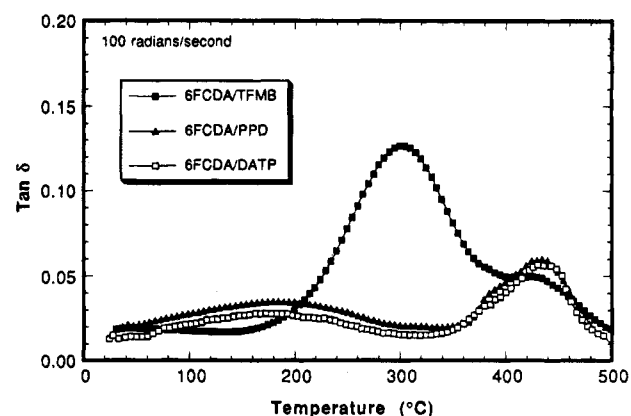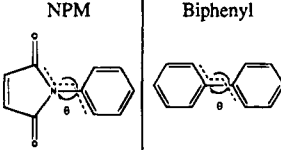
Both the temperature and magnitude of the subglass transition are significantly increased. As discussed earlier, these increases are attributed to steric effects of the 2,2'-trifluoromethyl substituents on the benzidine. The lack of change in the subglass relaxation by changes in the number of phenyl groups in the diamine moiety (at least for one or three phenyl groups) is attributed to the fact that simply increasing the number of rings along the backbone does not change the local environment affecting the rotation of phenyl groups responsible for the subglass relaxation. The rotational barrier in unsubstituted biphenyl is low—around 2 kcal/mol (Table 5). This is comparable to that in *N*-phenylmaleimide. It appears likely that the mechanism of the subglass relaxation in PPD and DATP is different from that in the substituted biphenyls.

The influence of backbone chemistry on the relaxation behavior in polyimides has been explored previously.[16,31-36] The glass transition is affected by the stiffness and linearity of the polyimide backbone. Increasing the stiffness generally increases the glass transition temperature, while increasing the linearity decreases the magnitude of the glass process. Polyimides made with rigid dianhydride and diamine comonomers generally do not exhibit prominent glass relaxations and have relatively high glass transition temperatures.[33] Because of the stiffness and linearity of the dianhydrides and diamines, the glass transition temperatures are high in all the polyimides in this study, near or above 400 °C. The only exception is the polyimide with the BPDA dianhydride, which has a relatively prominent glass transition at 340 °C. The single "crankshaft" bond between the two anhydride

**Table 5. Rotational Barriers (ΔE) in kcal/mol of
N-Phenylmaleimide (NPM) and Biphenyl**

	NPM	Biphenyl
Semi-Empirical MNDO/AM1		
θ_{opt} (°)	26	41
ΔE at $\theta = 0°$	0.61	2.10
ΔE at $\theta = 90°$	2.18	1.04
Local Density Functional Theory		
θ_{opt} (°)	53	43
ΔE at $\theta = 0°$	1.43	1.81
ΔE at $\theta = 90°$	1.34	2.61

Figure 12. 180° dihedral angle for disubstituted biphenyl.

Figure 13. Relative energies as a function of dihedral angle for 2,2'-dichlorobiphenyl as calculated by semiempirical molecular orbital theory (MNDO/AM1).

linkages in BPDA enhances the flexibility and accounts for the increase in magnitude in and lower temperature for the glass relaxation.

The subglass relaxation in most polyimides occurs between 50 and 200 °C. Unlike the glass relaxation, the subglass relaxation in polyimides is generally unaffected by the backbone stiffness or linearity. The subglass relaxation has been attributed to localized motion within the diamine moiety.[15,38] This is supported by the relatively low activation energies (Tables 1 and 2) characteristic of noncooperative localized motion.[37] The nature of the subglass relaxation has generally been explained in terms of rotation or oscillations of the phenyl groups within the diamine moiety of the polyimide. As reported here, the subglass relaxation in the polyimides based on TFMB is more prominent and occurs at a much higher temperature than typically observed in polyimides. In a kinetic sense, the presence of the CF_3 side groups on the 2,2'-positions of the benzidine moiety severely restricts the subglass relaxation, shifting the transition to much higher temperatures. In a thermodynamic sense, the presence of the CF_3 groups increases the magnitude of the relaxation. The CF_3 side groups sterically hinder the rotation of the phenyl groups about the polyimide backbone. According to Arnold et al.,[10] the steric hindrance of the CF_3 side groups significantly restricts the motion, permitting only limited oscillation about the backbone of the TFMB moiety. However, this explanation of extremely limited motion does not account for the prominence of the subglass relaxation.

Computer Modeling

Computer modeling was used to clarify the nature of the subglass relaxation. Butta et al.[39] attributed the subglass transition to "rotational vibrations" about quasi-equilibrium positions in the biphenyl and imide rings. More recently, Arnold et al.[10] concluded from molecular mechanics modeling that such "rotational vibrations" are not significant. Indeed the 2,2'-substituted diamines are said to be "almost locked-in" at the dihedral angles of 90 and 270°.

We investigated the rotational barrier of substituted biphenyls at dihedral angles of 180° (see Figure 12) by using electronic structure methods. Both semiempirical molecular orbital and density functional calculations were performed. Because semiempirical methods are
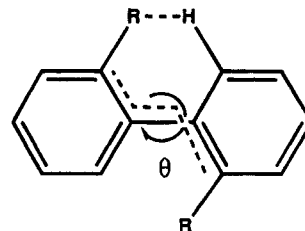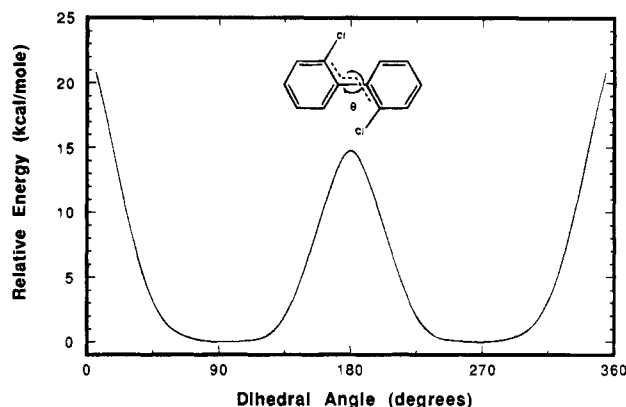
fast and inexpensive, they were performed for all substituents. Density functional calculations on the Cl, CH_3, CF_3, and OCF_3 substituents confirmed the trends seen in the semiempirical results.

The typical dependence of potential energy on dihedral angle is shown in Figure 13. The minimum-energy geometries of the substituted biphenyls have dihedral angles ranging from 100 to 145° (see Table 3). As the dihedral angle decreases from its minimum-energy value through 90° the energy increases slowly, giving a fairly broad potential energy "valley". As the dihedral angle approaches 0°, the energy increases substantially due to a large steric interaction; the substituents in the 2,2' positions are too close to each other. As the substituted biphenyl is rotated closer to $\tau = 0°$, each chlorine atom is forced out of the plane of the phenyl ring to which it is attached. Because of this distortion of the structure, the SCF equations fail to converge below $\tau = 3°$. One can infer that the energy at $\tau = 0°$ must be very high. A rigid rotation of the minimum-energy structure to $\tau = 0°$ gives a fully planar molecule with a Cl—Cl distance of 1.38 Å. The two chlorine atoms are clearly strongly overlapping. This is not the case for the 6,6' hydrogens. As the dihedral angle increases from its minimum-energy value, another rotational barrier is encountered with a maximum at 180°, where both substituents have steric interactions with hydrogen atoms in the 6 and 6' positions. This barrier is on the order of 10 kcal/mol (see Table 4) and is low enough to make rotational transitions important in some cases.

Our torsional potential can be contrasted to that reported by Arnold et al.[10] in their Figure 10, which shows infinitely high energy barriers at 0 and 180° and rather narrow wells centered at 90 and 270°. This descrepancy led us to further investigate the application of molecular mechanics to the rotational barriers in these systems. Computational results were obtained with the DISCOVER program from Biosym Technologies, Inc., with their CFF91 force field.[40-42] The results are shown in Figure 14. By comparison with Figure 13,
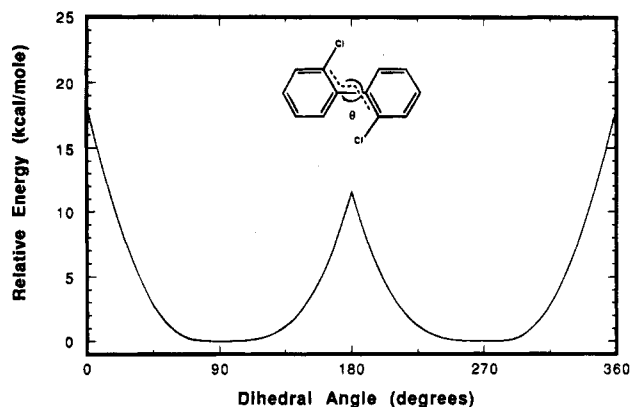
Figure 14. Relative energies as a function of dihedral angle for 2,2′-dichlorobiphenyl as calculated by molecular mechanics (DISCOVER/CFF91).

Table 6. Comparison of T_β (°C) and Semiempirical Rotational Energy Barriers (ΔE) in kcal/mol for Fluorinated Ether Substituents

	T_β	ΔE^a
OCF$_3$	138	8.0
OC$_2$F$_4$H	180	8.7
OC$_2$F$_3$HOC$_3$F$_7$	215	9.1

^{a} ΔE = difference in energy between the minimum-energy structure and the structure with a dihedral angle of 180°.

one can see that the major features of the rotational potential are correct, as is the magnitude of the barrier—ca. 10 kcal/mol. Molecular mechanics can be a viable approach to investigating these systems, but selection of an appropriate force field is critical. Furthermore, it is important to allow for geometry relaxation at the transition states. Rigid rotation from the minimum-energy structure leads to a barrier at 180° of 50.5 kcal/mol for 2,2′-dichlorobiphenyl when calculated using MNDO/AM1.

Table 4 shows the relationship between the subglass relaxation and the rotational barrier at 180° for OCF$_3$, Cl, CH$_3$, and CF$_3$. Both the semiempirical (AM1) and local density functional theory (LDFT) results show the same trend—the higher the barrier, the higher the subglass transition temperature. This trend, although suggestive, does not account for all of the observations.

Table 6 shows the semiempirical rotational barriers and subglass transition temperatures for the three fluorinated ether substituents. As one would expect, the free-molecule rotational barriers of the three biphenyls are roughly the same. (The side chains are flexible enough to move well away from the phenyl rings.) However, their subglass transition temperatures vary widely. This suggests that interactions between different polymeric chains are important. This is consistent with the result that the subglass transition temperature increases with length of the substituent.

Rotational barriers in the imide model compound *N*-phenylmaleimide and in biphenyl were also investigated. As shown in Table 5, both are much lower than the barriers in the substituted biphenyls—ca. 2 kcal/mol vs 10 or more kcal/mol.

The two unsubstituted p-aromatic diamines do not fit this simple model. Bi-phenyl has no possibility of internal rotation whereas the rotational barrier for the center ring of *p*-terphenyl is low—around 2 kcal/mol per ring—ring bond. However, as Table 2 shows, their subglass transition temperatures are near the average of those measured—roughly the same as for CH$_3$ or
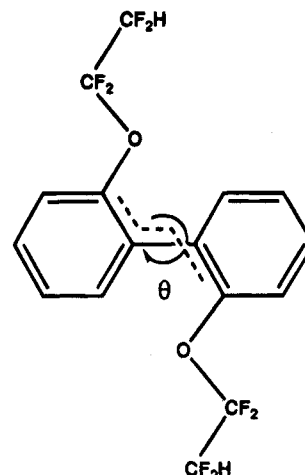

Figure 15. 2,2′-OCF$_2$CF$_2$H-disubstituted biphenyl showing how the ether linkage allows the alkyl groups to move away from aromatic rings.

O(C$_2$F$_4$H). This suggests that some mechanism other than internal rotation is responsible for the subglass relaxation in these materials.

Conclusions

The mechanical relaxation behavior of a series of stiff, highly rodlike polyimides based on 2,2′-disubstituted benzidines was investigated. Due to the rigid and highly rodlike nature of these polyimides, the glass relaxation occurs at high temperatures and is relatively weak. The subglass relaxation in these polyimides, on the other hand, is very prominent. The presence of CF$_3$ groups in the 2,2′-positions of the benzidine moiety increases the temperature approximately 150 °C and increases the magnitude of the subglass relaxation. The CF$_3$ groups sterically hinder the rotation of the phenyl groups about the polyimide backbone. Incorporating a flexible linkage (in this case oxygen) between the phenyl groups and the CF$_3$ side groups substantially reduces the impact of the side groups on the subglass transition temperature and to some extent the magnitude of the subglass relaxation. Changes in the number of p-aromatic groups within the rodlike diamine segment apparently do not significantly affect the glass or subglass relaxation behavior. The subglass relaxation is attributed to rotation of the phenyl groups in the benzidine moiety. Rotational barrier heights, obtained from quantum mechanical modeling for phenyl group rotation in the benzidine moiety along the polymer backbone, are comparable to values obtained from dynamic mechanical measurements of the subglass relaxation.

References and Notes

(1) Auman, B. C. In *Advances in Polyimide Science and Technology*; Feger, C., Khojasteh, M., Htoo, M., Eds.; Technomic Publishing: Lancaster, PA, 1993; Chapter 15.
(2) Feiring, A. E.; Auman, B. C.; Wonchoba, E. R. *Polym. Prepr. (Am. Chem. Soc., Div. Polym. Chem.)* **1993**, *34(1)*, 393.
(3) Feiring, A. E.; Auman, B. C.; Wonchoba, E. R. *Macromolecules* **1993**, *26*, 2779.

(4) Auman, B. C.; Trofimenko, S. *Polym. Prepr. (Am. Chem. Soc., Div. Polym. Chem.)* **1992**, *33(2)*, 244.

(5) Rogers, H. G.; Gaudiana, R. A.; Hollinsed, W. C.; Kalyanaraman, P. S.; Manello, J. S.; McGowan, C.; Minns, R. A.; Sahatjian, R. *Macromolecules* **1985**, *18*, 1058.

(6) Harris, F. W., Hsu, S. L.-C., Tso, C. C. *Polym. Prepr. (Am. Chem. Soc., Div. Polym. Chem.)* **1990**, *31(1)*, 342.

(7) Matsuura, T.; Hasuda, Y.; Nishi, S.; Yamada, N. *Macromolecules* **1991**, *24*, 5001.

(8) Matsuura, T.; Ishizawa, M.; Hasuda, Y.; Nishi, S. *Macromolecules* **1992**, *25*, 3540.

(9) Matsuura, T.; Yamada, N.; Nishi, S.; Hasuda, Y. *Macromolecules* **1993**, *26*, 419.

(10) Arnold, F. E., Jr.; Bruno, K. R.; Shen, D.; Eashoo, M.; Lee, C.; Harris, F. W.; Cheng, S. Z. D. *Polym. Eng. Sci.* **1993**, *33(21)*, 1373.

(11) Eashoo, M.; Shen, D.; Wu, Z.; Lee, C. J.; Harris, F. W.; Cheng, S. Z. D. *Polymer* **1993**, *34(15)*, 3209.

(12) Porter, R. S.; Zachariades, A. E.; Cheng, S. Z. D.; Wu, Z.; Eashoo, M.; Hsu, S. L.-C.; Harris, F. W. *Polym. News* **1991**, *16*, 49.

(13) Hougham, G.; Tesoro, G.; Shaw, J. *Macromolecules* **1994**, *27*, 3642.

(14) Ikeda, R. M. *J. Polym. Sci., Polym. Lett. Ed.* **1966**, *4*, 353.

(15) Bernier, G. A.; Kline, D. E. *J. Appl. Polym. Sci.* **1968**, *12*, 593.

(16) Perena, J. M. *Angew. Makromol. Chem.* **1982**, *106*, 61.

(17) Trofimenko, S. In *Advances in Polyimide Science and Technology*; Feger, C., Khojasteh, M., Htoo, M., Eds.; Technomic Publishing: Lancaster, PA, 1993; Chapter 3.

(18) Auman, B. C. *Polym. Prepr. (Am. Chem. Soc., Div. Polym. Chem.)* **1993**, *34(1)*, 443.

(19) McCrum, N. G.; Read, B. E.; Williams, G. *Anelastic and Dielectric Effects in Polymeric Solids*; Wiley: London, 1967.

(20) Dewar, M. J. S.; Theil, W. *J. Am. Chem. Soc.* **1977**, *99*, 4899.

(21) Thiel, W. *J. Mol. Struct.* **1988**, *163*, 415.

(22) Dewar, M. J. S.; Zoebisch, E. G.; Healy, E. F.; Stewart, J. J. P. *J. Am. Chem. Soc.* **1985**, *107*, 3902−3909.

(23) Andzelm, J.; Wimmer, E.; Salahub, D. R. In *The Challenge of d and f electrons: Theory and Computation*; Salahub, D. R., Zerner, M. C., Eds.; ACS Symposium Series 394; American Chemical Society: Washington, DC, 1989, p 228.

(24) Andzelm, J. In *Density Functional Methods in Chemistry*; Labanowski, J., Andzelm, J., Eds.; Springer-Verlag: New York, 1991; p 191.

(25) Andzelm, J. W.; Wimmer, E. *J. Chem. Phys.* **1992**, *96*, 1280. DGAUSS is a density functional program available via the Cray UniChem project.

(26) Vosko, S. H.; Wilk, L.; Nusair, M. *Can. J. Phys.* **1980**, *58*, 120.

(27) Perdew, J. P. *Phys. Rev.* **1986**, *B33*, 8822.

(28) Becke, A. D. *Phys. Rev.* **1988**, *A38*, 3098.

(29) Becke, A. D. In *The Challenge of d and f electrons: Theory and Computation*; Salahub, D. R., Zerner, M. C., Eds.; ACS Symposium Series 394; American Chemical Society: Washington, DC, 1989; p 166.

(30) Becke, A. D. *Int. J. Quantum Chem. Quantum Chem. Symp.* **1989**, *23*, 599.

(31) Coulehan, R. E.; Pickering, T. L. *Polym. Prepr. (Am. Chem. Soc., Div. Polym. Chem.)* **1971**, *12(1)*, 305.

(32) Gillham, J. K.; Hallock, K. D.; Stanknicki, S. J. *J. Appl. Polym. Sci.* **1972**, *16*, 2595.

(33) Gillham, J. K.; Gillham, H. C. *Polym. Eng. Sci.* **1973**, *13(6)*, 447.

(34) Gillham, J. K.; Gillham, H. C. *Org. Coat. Plast. Chem.* **1973**, *33(1)*, 201.

(35) Cooper, S. L.; Mair, A. D.; Tobolsky, A. V. *Text. Res. J.* **1975**, *35*, 1110.

(36) Fryd, M. In *Polyimides*; Mittal, K. L., Ed.; Wiley: New York, 1984; Vol. 1, p 377.

(37) Starkweather, H. W., Jr. *Polymer* **1991**, *32*, 2443.

(38) Kochi, M.; Shimada, H.; Kambe, H. *J. Polym. Sci., Polym. Phys. Ed.* **1984**, *22*, 1979.

(39) Butta, E.; de Petris, S.; Pasquoni, M. *J. Appl. Polym. Sci.* **1969**, *13*, 1073.

(40) Maple, J. R.; Hwang, M.-J.; Stockfisch, T. P.; Dinur, U.; Waldman, M.; Ewig, C.; Hagler, A. T. *J. Comput. Chem.* **1994**, *15(2)*, 162−182.

(41) Hwang, M.-J.; Stockfisch, T. P.; Hagler, A. T. *J. Am. Chem. Soc.* **1994**, *116*, 2515−2525.

(42) Sun, H.; Mumby, S. J.; Maple, J. R.; Hagler, A. T. *J. Am. Chem. Soc.* **1994**, *116*, 2978−2987.